LAUTECH Journal of Engineering and Technology 18 (1) 2024: 145-160

OPTIMIZATION OF MECHANICAL AND TRIBOLOGICAL PROPERTIES OF AL COMPOSITES REINFORCED WITH SELECTED AGRICULTURAL WASTE ASH FOR LIGHTWEIGHT ENGINEERING APPLICATIONS

[1]Asafa T. B., [1*]Osunmakinde L, [2]Agboola P. O. and [1]Durowoju M. O.

[1]Mechanical Engineering Department, Ladoke Akintola University of Technology, Ogbomoso, Nigeria.
[2]Mechanical Engineering Department, School of Science and Mathematics, Howard Payne University, Brownwood, TX 76801, USA
**Corresponding author: Osunmakinde L (labaikaosunmakinde@yahoo.com)*

ABSTRACT

Agricultural residues have been applied as reinforcements in metal matrix composites because of their low cost and the possibility of reducing environmental pollution. In most of these applications, the mixing ratios follow a parametric approach making optimization important for maximum deployment of agricultural residue. In this study, tribological and mechanical properties of Al composites reinforced with coconut shell ash (CSA), rice husk ash (RHA), and cassava peel ash (CPA) were optimized following a multi-objective optimization technique. Eleven samples were prepared in a two-step stair casting technique with the selected filler at 15wt.% and 85wt.% Al-powder as the matrix. The tensile strength, percentage elongation, wear rate, and elastic modulus of all synthesized samples were analyzed. The results show that the samples containing 5wt.%RHA + 5wt.%CSA + 5wt.%CPA + 85wt.%Al and 10wt.%RHA + 2.5wt.%CSA + 2.5wt.%CPA + 85wt.%Al gave optimum mechanical values (133.106 MPa, 8.175%, and 109.945 GPa) while samples with 2.5wt.%RHA + 10wt.%CSA + 2.5wt.%CPA + 85wt.%Al gave optimum wear rate (0.074Ml/Nm). Statistical analysis showed that the three fillers (RHA, CSA, and CPA) are significant implying that they are responsible for the variation in physicomechanical properties of the composites. The optimum physico-mechanical properties were 133.106 MPa, 8.175%, 109.945 GPa, and 0.074Ml/Nm and obtained at proportions of 5wt.%RHA + 5wt.%CSA + 5wt.%CPA + 85wt.%Al and 10wt.%RHA + 2.5wt.%CSA + 2.5wt.%CPA + 85wt.%Al and 2.5wt.%RHA + 10wt.%CSA + 2.5wt.%CPA + 85wt.%Al.

Keywords: *CSA; RHA; CPA; double stir casting; composites; and behavior.*

INTRODUCTION

Aluminum matrix composites reinforced with agro-wastes have been generally accepted in the automotive, aerospace, oil and gas, sport, and construction industries due to their excellent strength-to-weight ratio, good corrosion resistance, improved thermal coefficient of expansion, energy efficiency, low production cost, and lightweight (Atiqah, 2012; Alaneme *et al*., 2015; Hammar *et al*., 2020). Previous studies have shown that aluminum composites require minimal processing techniques, and are economically sustainable (Joseph *et al*., 2019). They reduce environmental pollution, are eco-friendly, energy efficient, have good homogenous reactions between the particles and matrix, and have perfect interfacial bonding (Tiwari et al., 2017; Ajayi *et al*., 2023). The performance of composites depends on the type and quantity of reinforcements, their weight ratio, wettability with matrix alloy, the processing method chosen, and the metallurgical properties of the matrix material (Aigbodion *et al*., 2020; Agbeleye *et al*., 2020; Ikubanni *et al*., 2021).

The incorporation of ceramic or synthetic particles as reinforcement in aluminum matrix composites has been shown to improve their stiffness, specific

strength, and wear resistance (Zuhallawati *et al*.,2007; Bannaravuri et al., 2018). However, this enhancement is accompanied by increased composite density, brittleness, reduced machinability, and a decline in fracture toughness (Baradeswaran *et al*., 2014; Kanthavel *et al*., 2016). These changes can lead to a reduction in composite impact strength due to decreased strain energy and the creation of regions of stress concentration (Adebisi *et al*., 2016). Furthermore, the production cost of aluminum matrix composites (AMCs) reinforced with synthetic materials can limit their availability and utilization, particularly in developing regions such as Africa (Dinaharan *et al*., 2017).

To address these shortcomings, utilizing agro-waste as a reinforcing agent has emerged as a promising alternative. Micheal et al. (Micheal *et al*., 2022) developed a hybrid aluminum composite (AA6061) reinforced with micro and nanoparticles of SiC and carbonized coconut shell (CSA) at varying proportions ranging from 0 to 15 wt.%. Their study demonstrated a progressive enhancement in mechanical properties, including tensile and yield strength, with the addition of particles to the matrix alloy. At a 15wt.% proportion of micro-particle reinforcement with CSA, an 8.5% improvement compared to unreinforced Al-alloy was observed. Similarly, Dwivedi *et al*., (2020) produced a hybrid aluminum composite using a stir casting technique and reinforced the alloy with SiC and rice husk ash (RHA) at a 15wt.% proportion. Optimal tensile strength was achieved at a proportion of 12.5wt.% SiC and 2.5wt.% RHA, although an increase in RHA content led to a degradation in tensile strength. The ductility and fracture toughness of the composites decreased with increasing weight ratio of SiC and RHA up to 15wt.%, while the composite hardness peaked at 15wt.% SiC and 0wt.% RHA.

In addition, Olanira *et al*.,(2020) investigated an Al-hybrid composite reinforced with SiC and cassava peel ash (CPA) at various proportions (100:0, 75:25, and 50:50). Their analysis revealed a progressive improvement in composite hardness and tensile strength as the reinforcement ratio increased. However, the fracture toughness and impact energy of the composite were negatively affected. Similarly, other researchers have explored different reinforcement materials and techniques. Varalakshmi *et al*., (2019) reinforced Al6061 with CSA using stir casting, while Prasad et al., (2014) employed RHA and SiC for double stir casting of Al-composites. Aigbodion and Hassan, 2015 synthesized Al-Cu-Mg composites with eggshells as a reinforcement.

Most studies conducted on particulate-reinforced aluminum composites focus on the influence of the proportion of the reinforcing agent on the properties of the aluminum alloy. However, there has been limited investigation into the effects of both particle proportion and particle size. Furthermore, only a small number of studies have attempted to model the properties of aluminum hybrid composites as a function of particle proportion using selected agro-waste particles. Hence, this study explored the impact of rice husk ash (RHA), carbonized coconut shell ash (CSA), and cassava peel ash (CPA) on aluminum hybrid composites, to model the experimental outcomes using design expert software. Rice husk, coconut shell, and cassava peel were chosen based on their availability (Mdakson *et al*., 2012; Gladston *et al*., 2017; Naim Shaik *et al*., 2019).

MATERIALS AND METHOD

Materials

Local sources of cassava peel and rice husk included gari and rice processing mills; coconut shells came from a local Ogbomoso market in Oyo state, Nigeria. Following the procedure outlined by

Osunmakinde *et al*., (2023), these agricultural wastes were dried, screened to remove undesirable particles, and processed into ash particles. The study's matrix material, 98% pure aluminum powder, was obtained from Loba Chemie PVT LTD in India. Table 1 displays the elemental composition of the calcined agricultural waste and the matrix alloy.

Table 1: Elements in the aluminum powder alloy and chemical oxides in RHA, CSA, and CPA.

Constituents	**Si**	**Cu**	**N**	**Fe**	**Mn**	**Ti**	**Al**			
Al-alloy %	0.1	0.02	0.001	0.1	0.02	0.03	Bal			
Constitutents	**SiO_2**	**Al_2O_3**	**Fe_2O_3**	**CaO**	**MgO**	**Na_2O**	**K_2O**	**SO_3**	**P_2O_5**	**C**
RHA %	91.73	1.56	0.16	1.16	0.47	-	0.73	-	-	1.13
CSA %	45.46	15.65	12.73	0.75	15.81	0.42	-	-	0.02	-
CPA %	36.75	7.71	2.60	8.29	2.9	1.34	18.68	1.58	-	-

Synthesis Of Composite

Due to its cost-effectiveness, a two-step stir casting method was employed to fabricate the aluminum matrix composite. An initial charge calculation was performed to ascertain the necessary amounts of 15%wt ash particles and Al-alloy for composite fabrication, as shown in Table 2. An Al-Si-Fe-containing pure aluminum powder was added to a graphite crucible furnace. The Al alloy was fully melted by heating the furnace to a regulated temperature of 710 ± 20°C (Alaneme *et al*., 2015) using a fuel-fired furnace.

In the meantime, the preheated ash particles were heated to 250°C for three hours to eliminate moisture and enhance the wettability of the particles with the matrix during the melting. Upon reaching the desired temperature, the preheated ash particles were introduced into the partially solidified melt and vigorously mixed by hand for five to ten minutes to prevent agglomeration, resulting in the formation of a slurry. Subsequently, the slurry was superheated to 780 ± 30°C, and further stirred for 8 minutes at 500 rpm using an automated stainless-steel stirrer to achieve homogeneity within the melt. Following this, the molten mixture was cast into a pre-prepared sand mold and allowed to solidify, resulting in the formation of the aluminum matrix composite.

Mechanical Properties

A tensile test was conducted on the samples using a Tensiometer. Prior to the test, samples of dimensions of 6 mm diameter and 20 mm gauge length were machined from the as-cast composites (Figure 1) using Instron lathe machine following ASTM E8/E8M-16ae1 standard. Each sample was securely clamped onto the tensiometer and subjected to monotonic tension until fracture occurred at room temperature (ASTM E8/E8M-16ae1, 2016). To ensure data reliability, three replicate tests were performed on each composite sample. From the results, tensile strength, percentage elongation, and elastic modulus were extracted.

Table 2. Sample designation and reinforcements weight ratio

Sample designation	Composition
1	Al-alloy
2	Al-alloy + 10% CSA + 2.5%CPA + 2.5%RHA
3	Al-alloy + 7.5% CSA + 7.5%CPA + 0%RHA
4	Al-alloy + 7.5 % CSA + 0% CPA + 7.5% RHA
5	Al-alloy +2.5% CSA + 2.5% CPA + 10% RHA
6	Al-alloy + 0% CSA + 15% CPA + 0% RHA
7	Al-alloy + 15% CSA + 0% CPA + 0% RHA
8	Al-alloy + 5% CSA + 5% CPA + 5% RHA
9	Al-alloy + 0% CSA + 0% CPA + 15% RHA
10	Al-alloy + 2.5% CSA +10% CPA +2.5%RHA
11	Al-alloy + 0% CSA + 7.5% CPA + 7.5% RHA

Wear Characterization

A Rotopol-V tribometer was used to examine the wear loss of the samples following the (ASTM G99-05 standard, 2010). Samples of length 40 mm and diameter 10 mm were prepared on lathe. The samples were subjected to a load of 20 kg at a sliding speed of 1.5 m/s. The wear rate was calculated from the weight loss and time of contact.

Fig.1: Samples of composites reinforced with CSA/CPA/RHA using a two-step stair casting method.

RESULTS AND DISCUSSION

Mechanical Behavior

Tensile strength, percentage elongation, and elastic modulus: According to Fig. 2, samples were grouped into four different categories; sample A represents unreinforced alloy while samples reinforced with a single ash particle, two distinct ash particle and three ash particles are designated as B, C and D, respectively.

Aside from the control samples, there was a notable progressive enhancement observed in the composite tensile properties. Group B exhibited a 59.88% enhancement, Group C showed a 65.69% improvement, and Group D displayed a 78.86% enhancement compared to the unreinforced alloy. The combination of three different agro-waste ash particles yielded the highest enhancement; however, the use of single and duo combinations also provided significant reinforcement to the alloy.

This observation aligns with previous studies by (Oghenevweta and Aigbodion 2016; Ahmed *et al.*, 2016; Osunmakinde *et al*., 2023; Adesina *et al*., 2023) where agro-waste ash was applied as either primary or secondary filler in the production of hybrid Al-composites. There are several reasons for the observed increase in sample strength.

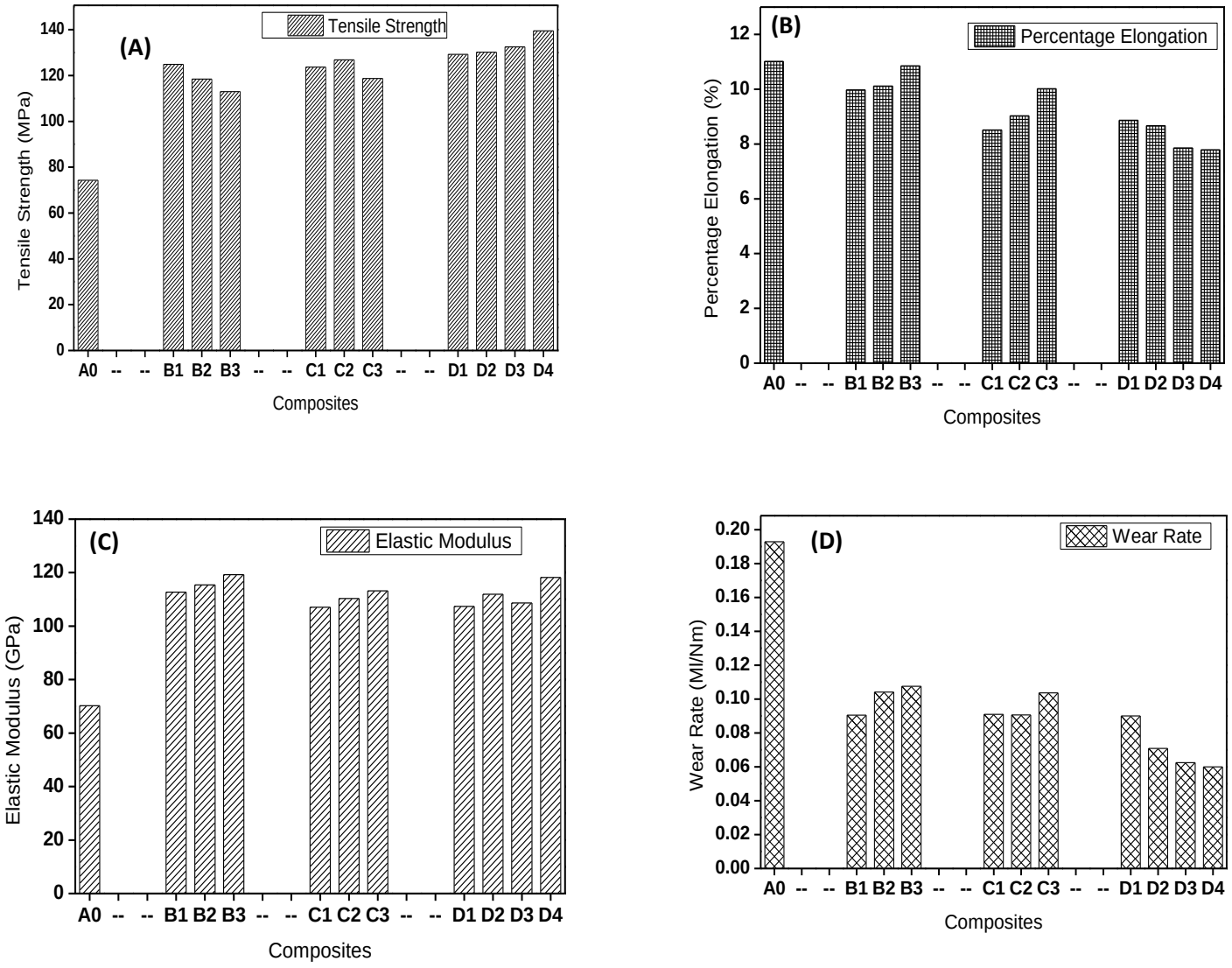

Fig.2: (A) plotted tensile strength of synthesized composites, (B) plotted percentage elongation of synthesized composites, (C) plotted elastic modulus of synthesized composites, and (D) plotted wear rate of synthesized composites.

First, the filler's incorporation of hard, brittle phases including SiO_2, Al_2O_3, and Fe_2O_3 and grain refinement at the matrix-particle contact hindered dislocation movement around grain boundaries, thereby increasing dislocation density within the grains. This, in turn, strengthened the soft Al-alloy, enhancing the composite's strength. Additionally, during cooling, a thermal mismatch resulted from the filler's and matrix's different coefficients of thermal expansion, impeding dislocation movement and indirectly strengthening the composite. Another mechanism contributing to composite strengthening is the capacity of the matrix to transmit load to the filler particles at the matrix-particle interface, strengthening the composite's ability to work harden and resist plastic deformation. At 139.47 MPa, the sample with the highest tensile strength was made up of 5 wt% RHA, 5 wt% CSA, 5 wt% CPA, and 85 wt% Al. This is explained by the presence of harder and more brittle phases, which increase the

composite's strength even further. The results presented by (Prasad *et al.*, 2014; Alaneme *et al*., 2020; Saini *et al*., 2020) are in agreement with these findings.

However, the percentage elongation of the reinforced composite decreased with the tensile strength, as shown in Fig. 2b; as a result, the percentage elongation and the created composite's tensile strength are inversely related. In comparison to the matrix material, samples B, C, and D exhibit reductions in percentage elongation of 6.35%, 16.61%, and 24.68%, respectively. The improvement in the composite tensile strength, the existence of particle clustering at the particle-matrix interface, and the presence of hard and brittle phases in the composite may have contributed to the decrease in the percentage elongation of the samples. This observation aligns with the findings of (Aigbodion *et al*., 2010; Saravanan and Kumar, 2014). However, the elastic modulus of the composites behaved contrary to the percentage elongation of the synthesized composite, although there is an appreciable improvement compared to the unreinforced al-alloy but not align with the tensile strength result as a dosage of 15wt.% proportion of agro-waste ash was used as filler in the alloy. From Fig. 2c, composite reinforced with single ash possesses the highest elastic modulus, followed by sample reinforced with three different ash particles combined, and lastly the double ash particles reinforced composite as 64.85%, 58.81%, and 56.89% for B, D, and C respectively. This shows that the ash particle has a different elastic modulus value, for coconut shell ash is 512 GPa (Micheal *et al*., 2020), while for rice husk ash is around 70 GPa (Alaneme *et al*., 2015) which is similar to the al-alloy value. The hard and brittle phase alters the microstructure of the composite, with good interfacial bond at the particle-matrix interface and particle clustering fine-tuning the samples' elastic modulus. These observations were in tandem with previous researchers (Olaitan, 2013; Atuanya *et al*., 2014; Atuanya *et al*., 2015).

Wear rate: The wear result of the synthesized composite is presented in Fig. 2d. The result shows a reduction of 63.28%, 50.68%, and 47.79% from sample categories D, C, and B respectively as compared to the unreinforced matrix material. This could be attributed to the difference in the presence of aluminosilicate and ferric oxide in the reinforcement particles at 15wt.% proportion of dose used as a filler in the composite. In the absence of brittleness in the composite, the aluminosilicate and ferric oxide (SiO_2, Al_2O_3, and Fe_2O_3) also referred to as the "hard phase" reduce the composite's ductility and wear rate. The soft matrix surface is shielded from severe contact with the steel disc counterface by these hard phases. The particle-matrix interface's strong interfacial bonding increases plastic shear strain, which strengthens the composites' resistance to wear. These observations align with earlier researchers (Saravanan *et al*., 2013; Prasad *et al*., 2014; Kingsly *et al*., 2017; Virkunwar *et al.*, 2019). The samples reinforced with three different particles combined as a filler performed better than the rest in the composite.

Statistical Analysis: I, J, and K represent rice husk ash (RHA), coconut shell ash (CSA), and cassava peel ash (CPA) particles in the proportion of (wt%), tensile strength (MPa), percentage elongation (%), wear rate (Ml/Nm), and elastic modulus (GPa) were analyzed. Analysis of variance (ANOVA), and surface response analysis were used to analyze the experimental outcome of each of the responses under evaluation. Design Expert 13 software was used for the aforementioned analysis, and ANOVA was conducted at a 95% confidence level and 5% significance. Furthermore, the effect of mixed particles (variables: I, J, and K) significance was analyzed to ascertain their impact on the responses.

Table 3 shows the experimental outcome and responses of the combined parameters.

ANOVA: Analysis of variance for the tensile strength is presented in Table 4. The model (Eq. 1) is considered significant since $p < 0.05$, and the linear mixture is significant for the same reason. However, the interactions between variables IJ, IK, and JK are insignificant. The coefficient of determination (R^2) for the regression model is 0.9446, hence the model is statistically fit to represent the data. For the percentage elongation, ANOVA result is presented in Table 5. While the model (Eq. 2) is significant, the linear mixture is insignificant. The interaction between variables IJ and IK is significant while JK is insignificant. The coefficient of determination (R^2) for the regression model is 0.9145 indicating statistical fitness of the model.

Table 3: Experimental outcome and responses

	I	J	K	L	Response 1	Response 2	Response 3	Response 4
Run	I:RHA	J:CSA	K:CPA	L:Al	Tensile Strength	Percentage Elongation	Wear rate	Elastic Modulus
					MPa	%	Ml/Nm	GPa
1	0	0	0	100	74.27	11.02	0.19288	70.24
2	10	2.5	2.5	85	132.48	7.86	0.06242	108.65
3	7.5	7.5	0	85	123.65	8.52	0.09103	107.05
4	7.5	0	7.5	85	126.85	9.03	0.09068	110.35
5	2.5	2.5	10	85	129.25	8.87	0.08999	107.35
6	0	15	0	85	118.45	10.12	0.10406	115.4
7	15	0	0	85	124.85	9.98	0.09052	112.73
8	5	5	5	85	139.47	7.79	0.06	118.23
9	0	0	15	85	112.93	10.86	0.10752	119.25
10	2.5	10	2.5	85	130.15	8.67	0.07084	111.95
11	0	7.5	7.5	85	118.68	10.02	0.10367	113.2

Table 4: ANOVA results on tensile strength

Source	**Sum of Squares**	**df**	**Mean Square**	**F-value**	**p-value**	
Model	2778.38	6	463.06	11.36	0.0171	Significant
[(1)]Linear Mixture	2493.78	3	831.26	20.39	0.0069	
IJ	53.94	1	53.94	1.32	0.3141	
IK	161.10	1	161.10	3.95	0.1178	
IL	0.0000	0				
JK	72.76	1	72.76	1.78	0.2525	
JL	0.0000	0				
KL	0.0000	0				
Residual	163.10	4	40.78			
Cor Total	2941.49	10				

Table 5: ANOVA results on percentage elongation.

Source	Sum of Squares	df	Mean Square	F-value	p-value	
Model	11.56	6	1.93	7.13	0.0390	Significant
[(1)]Linear Mixture	4.62	3	1.54	5.70	0.0629	
IJ	3.33	1	3.33	12.31	0.0247	
IK	2.97	1	2.97	11.00	0.0295	
IL	0.0000	0				
JK	0.7116	1	0.7116	2.63	0.1800	
JL	0.0000	0				
KL	0.0000	0				
Residual	1.08	4	0.2703			
Cor Total	12.64	10				

Tensile Strength = +123.57I +117.86J +112.31K +74.27L +32.65IJ +56.42IK +0.0000IL

+37.92JK +0.0000JL +0.0000KL

R^2 = 0.9446 (1)

Percentage Elongation = +9.97I +10.22J +10.91K +11.02L -8.11IJ -7.76IK +0.0000IL

-3.75JK +0.0000JL +0.0000KL

R^2 = 0.9145 (2)

ANOVA table for the wear rate analysis is presented in Table 6, indicating that the model generated (Eq.3) is considered significant as $p < 0.05$, and the linear mixture is also significant. However, the interactions between variables IJ, IK, and JK are deemed insignificant. The coefficient of determination (R^2) for the regression model developed for percentage elongation is 0.9140, indicating that the model is statistically suitable for representing the fitted data. Similarly, ANOVA table for elastic modulus is presented in Table 7, demonstrating that the model generated (Eq.4) is significant since $p < 0.05$, and the linear mixture is also significant since. The cross-interactions between variables IJ, IK, and JK are found to be insignificant. The coefficient of determination (R^2) for the regression model developed for elastic modulus is 0.9406, indicating that model Eq.4 is statistically appropriate for representing the fitted data.

Table 6: ANOVA results on wear rate

Source	Sum of Squares	Df	Mean Square	F-value	p-value	
Model	0.0117	6	0.0020	7.08	0.0395	Significant
[(1)]Linear Mixture	0.0107	3	0.0036	12.88	0.0160	
IJ	0.0004	1	0.0004	1.57	0.2786	
IK	0.0004	1	0.0004	1.52	0.2856	
IL	0.0000	0				
JK	0.0002	1	0.0002	0.8054	0.4202	
JL	0.0000	0				
KL	0.0000	0				
Residual	0.0011	4	0.0003			
Cor Total	0.0128	10				

Table 7: ANOVA results on elastic modulus

Source	Sum of Squares	Df	Mean Square	F-value	p-value	
Model	1674.56	6	279.09	10.55	0.0195	Significant
[(1)]Linear Mixture	1644.50	3	548.17	20.73	0.0067	
IJ	14.75	1	14.75	0.5576	0.4967	
IK	11.97	1	11.97	0.4526	0.5380	
IL	0.0000	0				
JK	3.68	1	3.68	0.1390	0.7282	
JL	0.0000	0				
KL	0.0000	0				
Residual	105.80	4	26.45			
Cor Total	1780.35	10				

Table: Elastic modulus

$$\text{Wear rate} = +0.0906I +0.1040J +0.1124K +0.1929L -0.0924IJ -0.0909IK +0.0000IL -0.0662JK +0.0000JL +0.0000KL \quad R^2 = 0.9140 \quad (3)$$

$$\text{Wear rate} = +112.23I +115.29J +117.24K +70.24L -17.07IJ -15.38IK +0.0000IL -8.52JK +0.0000JL +0.0000KL \quad R^2 = 0.9406 \quad (4)$$

Surface and contour plot responses. Surface and contour plot responses illustrating the interactions among the three independent variables—rice husk ash, coconut shell ash, and cassava peel ash—are depicted in Fig. 3a, b, c, and d. In Fig. 3a, it is observed that proportions of variables I (rice husk ash), J (coconut shell ash), and K (cassava peel ash) range between 5.9117 and 6.3158wt.%, 4.7961 and 5.0394 wt.%, and 0.1381 and 0.2989 wt.%, respectively enhance the composite's tensile strength. However, proportions beyond these ranges have a detrimental effect on tensile strength. Optimum tensile strength is achieved below 6.3158, 5.0394, and 0.2989 wt.% for I, J, and K respectively.

In Fig. 3b, the interaction of ash particles I, J, and K results in a progressive reduction in the ductility of the composites. The ductility increases with increasing ash proportion but beyond certain thresholds, the ductility decreases (between 5.6455 and 6.2265 wt% for I, 0.5984 and 4.73116 wt% for J and between 0.8733 and 4.4251 wt% for K). Fig. 3c displays a similar pattern with an inverted "u" shape, indicating a reduction in the composite's wear rate as the ash proportions increase within certain ranges. Hence ash particle proportion ranged between 3.3008 and 15 wt.% for ash particle I, 4.4732 and 15wt.% for J, and 3.4760 and 15wt.% for K giving progressive enhancing effect on the composite.

In Fig. 3d, the interaction between variables I, J, and K significantly affects the elastic modulus of the composites. Synergetic effects are observed within certain ranges, while antagonistic effects are seen beyond those ranges. In Fig. 3d, the interaction and reaction of the variables' proportion have a significant effect on the composite elastic modulus, for variable I between 0.0326 and 11.2133wt.%, variable J between 0.0179 and 11.0065wt.%, and variable K between 0.0188 and 11.2292wt.% show synergetic effect on the composite. However, between 11.2133 and 15wt.%, 11.0065wt.%, and 11.2292 and 15wt.% resulted in an antagonistic effect on the composite. The result revealed that interaction among the variables on each experimental factor response is more pronounced than individual variable, although each variable made a significant effect on the experimental factor response.

The contour plots in Figure 4a-d indicate areas where each response can be optimized. Table 8 presents some parametric combinations of variables to achieve optimal responses. Further optimization for the resultant responses was conducted to optimize the mechanical properties as a single entity, resulting in predicted responses for tensile strength, percentage elongation, wear rate, and elastic modulus (Table 9). Fig.5 shows optimum condition as 7.73735wt%, 2.30613wt%, and 4.95652wt% for particle proportions I, J, and K, respectively. The predicted responses at these conditions are 133.106MPa, 8.17591%, 0.0736645Ml/Nm, and 109.946GPa for tensile strength, percentage elongation, wear rate, and elastic modulus respectively. However, the

validated results were obtained as 134.96MPa (-0.014% error), 7.82% (0.043% error), 0.0713Ml/Nm (0.036% error), and 111.02GPa (-0.010% error) for tensile strength, percentage elongation, wear rate, and elastic modulus, respectively. The validated results showed minimal errors, with models deemed significant (less than 5% prediction error). The composite developed under these optimized conditions could be suitable for various applications including automobile components, architecture, sports equipment, and lightweight engineering applications.

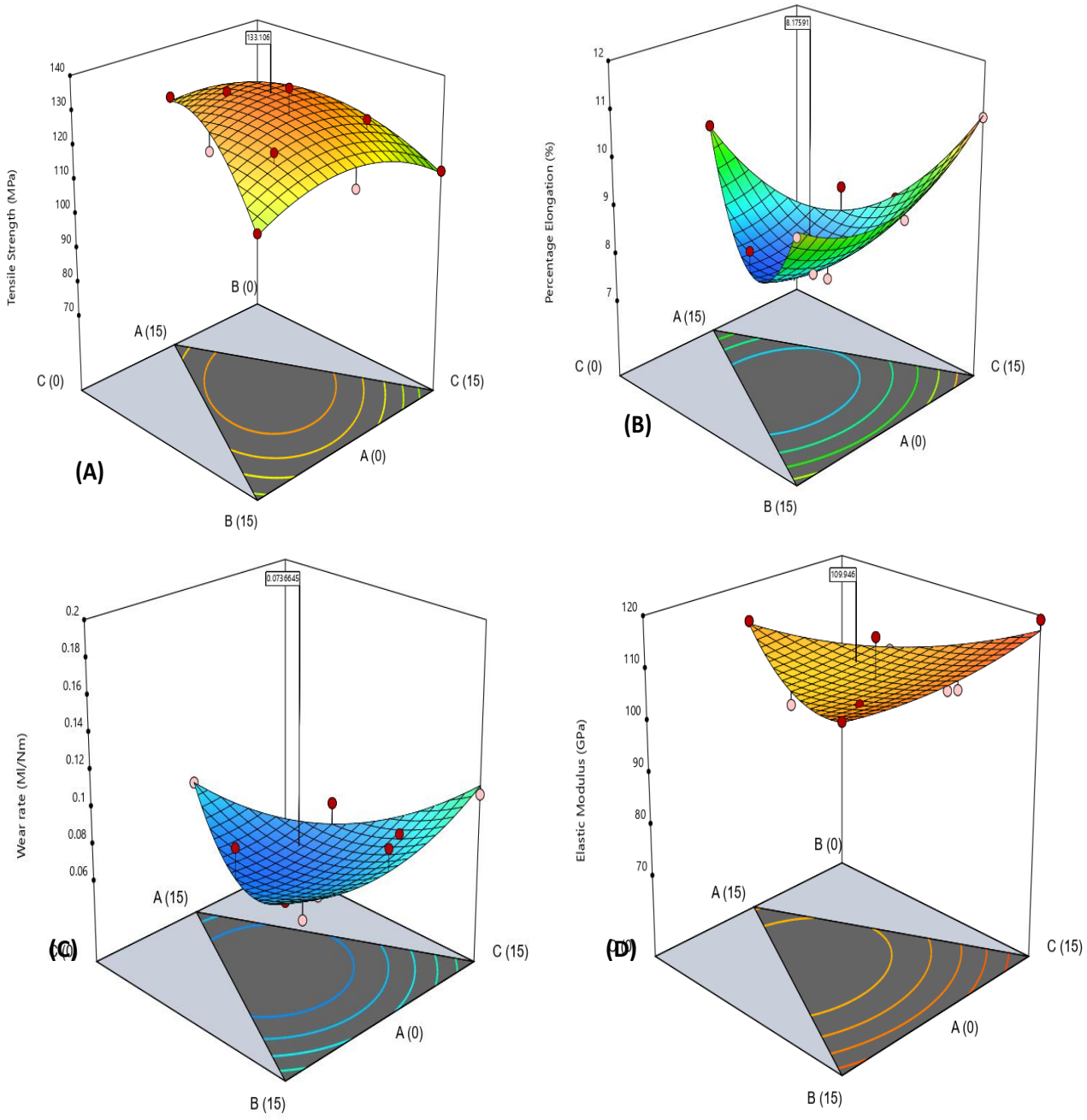

Fig. 3: Surface plots for the synthesized composites at 15wt.% proportion (A) tensile strength, (B) percentage elongation, (C) wear rate, and (D) elastic modulus. A=I is rice husk ash, B=J is coconut shell ash and C=K is cassava peel ash.

Table 8: The combined variables in attaining optimized response parameters

Response	Marked optimum	Ranged values for particle proportion (wt.%)			Predicted range of response	Predicted maximum response
		I	J	K		
Tensile strength	1	0 – 7.80	0 – 2.26	0 – 4.93	125 – 135 MPa	133.106 MPa
Percentage elongation	2	0 – 7.476	0 – 2.362	0 – 5.162	8.5 – 9.0 %	8.175 %
Wear rate	3	0 – 7.476	0 – 2.398	0 – 5.126	0.08–0.09Ml/Nm	0.074 Ml/Nm
Elastic modulus	4	0 – 7.590	0 – 2.370	0 – 5.040	114 – 116 GPa	109.945 GPa

Table 9: The optimization goals and range

Name	Goal	Lower limit	Upper limit	Lower weight	Upper weight	Importance
I: RHA	Ranged between	0	1	1	1	3
J: CSA	Ranged between	0	1	1	1	3
K: CPA	Ranged between	0	1	1	1	3
L: Al	Ranged between	85	100	1	1	3
Tensile strength	Ranged between	74.27	139.49	1	1	3
Percentage elongation	Ranged between	7.79	11.02	1	1	3
Wear rate	Ranged between	0.06	0.19288	1	1	3
Elastic modulus	Ranged between	70.24	119.25	1	1	3

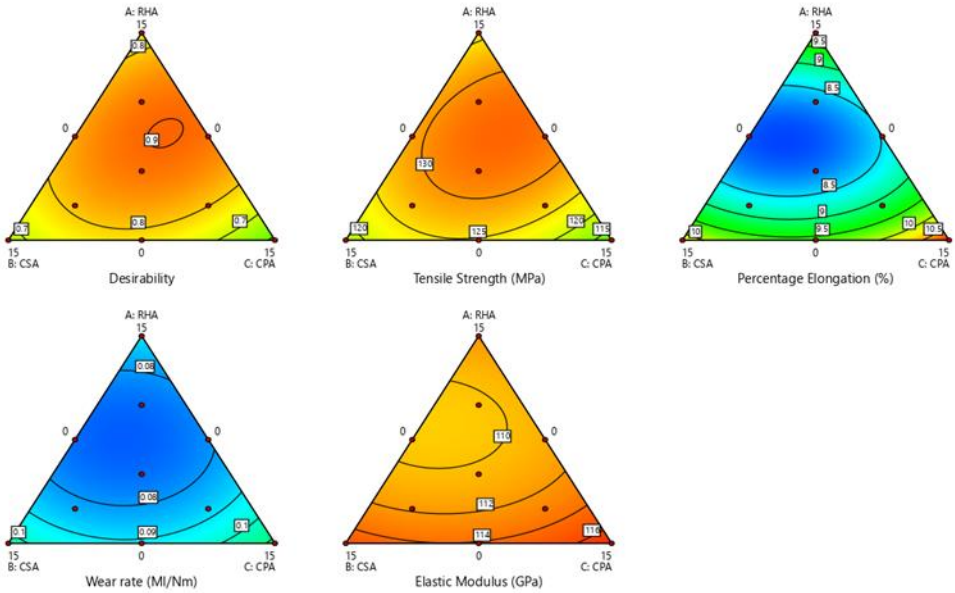

Fig. 4: contour plots for the synthesized composites at 15wt.% proportion (a) tensile strength, (b) percentage elongation, (c) wear rate, and (d) elastic modulus. A=I is rice husk ash, B=J is coconut shell ash and C=K is cassava peel ash.

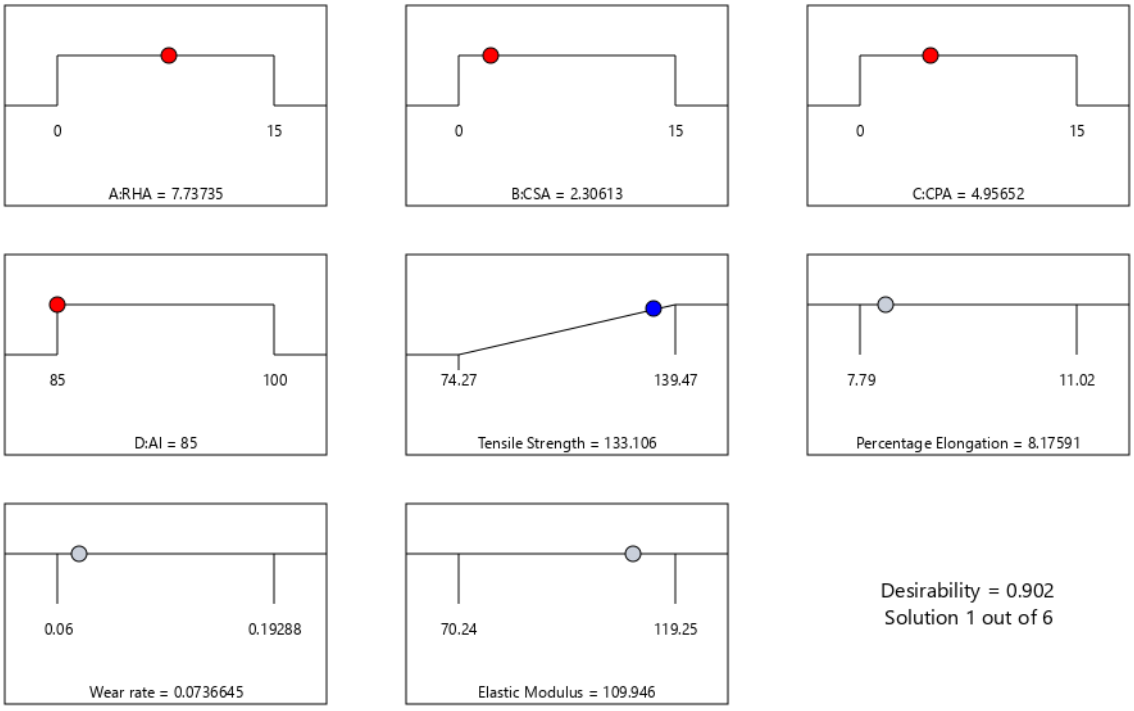

Fig. 5: Optimization ramp of responses.

CONCLUSIONS

The agro-waste ashes (RHA, CSA, and CPA) were used at different proportions as a filler in Al-hybrid composite for lightweight engineering applications. The mechanical properties of the sample composites were analyzed. The listed conclusions were made

- When compared to the unreinforced matrix, the sample composites' tensile strength

gradually rose. The highest tensile strength, however, is a result of combining three distinct ash particles, with samples 2 and 8 being inside the range of ideal tensile strength.

- The percentage elongation decreases progressively thereby reducing the composite ductility. It was observed that the influence of hard and brittle phases of the filler reduced the composite ductility.
- As the particle combination rose to three, the wear resistance of the composite increased at a 15% weight percentage. It was found that the filler's brittle, hard phases act as protuberances for the composite.
- The elastic modulus of all the composite samples was enhanced significantly with the application of 15wt.% proportion of selected agricultural waste particles ash.
- Experimental variables (RHA, CSA, and CPA) have significant contributions to the response as confirmed by the statistical analysis.

The regression models are statistically fit to represent the experimental outcome.

REFERENCES

Adebisi AA, Maleque A, Ali MY (2016) Effect of variable particle size reinforcement on mechanical and wear properties of 6061Al – SiC p composite. Compos InterfaCes 23:533–547.

Adesina O.S, Akinwande A.A, Balogun O.A, Adediran A.A, Sanyaolu O.O, and Romanovski V. (2023) Statistical analysis and optimization of the experimental results on performance of green Al7075 hybrid composites. Journal of Computer Science. DOI: 10.3390/jcs7030115.

Agbeleye AA, Esezobor DE, Balogun SA, Agunsoye JO, Solis J, and Nevile A (2020). Tribol- logical properties of aluminum -clay composites for brake disc rotor applications. J. King Saud Sci. 32:21-28.

Aigbodion V.S, Hassan S.B, and Oghenevweta J.E (2010) Microstructural analysis and properties of Al-Cu-Mg/bagasse ash particulate composites. J. Alloys Compd 497:188-94.

Ahmed AA, Ahmed R, Hossain MB, and Billah M (2016) Fabrication and characterization of aluminum-RHA composite prepared by stir casting method. Rajshahi Univ J Sci Eng 44:9-18.

Aigbodion, V.S, and Ezema, I.C (2020). Multifunctional A365 alloy/PKSAnp composites: microstructure and mechanical properties. Defense Technol. 16, 731-736.

Ajayi A.A, Mohan T.P, Kanny K, and Velmurugan R (2023) Thermal and wettability properties of nanoclay-filled epoxy-based foam composite as lightweight material. Journal of Materials Performance and Characterization. DOI: 10.1520/MPC20230085.

Alaneme K.K, Babalola S.A, Chown L.H, Bodunrin M.O (2020) Hot deformation behavior of bamboo leaf ash-silicon carbide hybrid reinforced al-based composite. Manuf Rev 17:1-14.

Alaneme, K.K and Sanusi, K.O (2015). Microstructural characteristics, mechanical and wear behavior of aluminum matrix hybrid composites reinforced with alumina, rice husk ash, and graphite. Engineering Science and Technology on International Journal 18, 416-422.

ASTM E8/E8M-16ae1 (2016). Standard test method for tension testing of metallic materials ASTM international.www.astm.org.

ASTM G99-05 (2010) Standard test method for wear testing with a pin-on-disk apparatus Conshohocken DOI:10.1520/G0099-05.

Atiqah, M (2012). Development and characterization of coir fibre reinforced composite brake friction materials. Arab J Sci Eng. 38: 3191-3199.

Atuanya C.U, Edokpta R.O, and Aigbodion V.S (2014) The physico-mechanical properties of recycled low-density polyethlene (RLDPE)/bean pod ash particulate composite. Res. Phys. 4(2)1-8.

Atuanya C.U, Aigbodion V.S, Obiorah S.O, Kchaou M, and Elleuch R (2015) Empirical model for estimating the mechanical and morphological properties of recycled low-density polyethylene/snail shell bio-composites. J. Assoc. Arab. Univ. Basic Appl. Sci. 5:1-9.

Bannaravuri, P.K and Birru, A. K (2018). Strengthening of mechanical and tribological properties of Al-4.5%Cu matrix alloy with the addition of bamboo leaf ash. Results In Physics10, 360-373.

Baradeswaran A, Perumal AE (2014) Study on mechanical and wear properties of Al7075 /Al2O3 / graphite hybrid composites. Compos Part B 56:464–471.

Dinaharan, I., Kalaiselvan, K., Murugan, N. (2017). Influence of rice husk ash particles on microstructure and tensile behavior of AA6061 aluminum matrix composites produced using friction stir processing. Composites Communications 3, 42–46.

Dwivedi S.P, Maurya N.K, Srivastava A.K, and Sahu R. (2020) Microstructure and mechanical behavior of Al/SiC/RHA hybrid metal matrix composite. international Information and Engineering Technology Association. DOI:10.18280/rcma.300107

Gladston, J.A.K., Dinaharan, I., Sheriff, N.M., Selvam, J.D.R. (2017). Dry sliding wear behavior of AA6061 aluminum alloy composites reinforced rice husk ash particulates produced using compo-casting. Journal of Asian Ceramic Societies 5(2), 127–135.

Hammar, I.K, Eko, S, and Dody, A. (2020). Investigation of industrial and agro-waste for aluminum matrix composite reinforcement. Procedia Structural Integrity, 6th ICIMECE 27, 30- 37.

Hassan SB, and Aigbodion VS (2015) Effects of eggshell on the microstructures and properties of Al-Cu-Mg/eggshell particulate composites. J King Saud Univ. Eng. Sci 27:49-56.

Joseph, O.O and Babremu, K.O (2019). Agricultural waste as a reinforcement particulate for Al metal matrix composites (AMMCs). A review. MDPI fibers 7,33.

Kanthavel K, Sumesh KR, Saravanakumar P (2016) Study of tribological properties on Al /Al2O3 / MoS2 hybrid composite processed by powder metallurgy. Alexandria Eng J 55:13–17.

Kingsly J.A, Dinaharan I, Sheriff N.M, and Raja J.D (2017) Sliding wear behavior of AA6061 alloy composites reinforced rice husk ash particulates produced using compocasting. J. Asian Ceram. Soc. 5:127-135 https://doi.org/1016/j.jascer.2017.03.005.

Madakson, P.B., Yawas, D.S., Apasi, A. (2012). Characterization of Coconut Shell Ash for potential utilization in metal matrix composites for automotive applications. International Journal of Engineering Science and Technology 4(3), 1190–1198.

Micheal, N.N, Umoru E.L, and Youngson, N.U (2022). Comparative study of tensile properties of hybrid AA6061/SiC/Carbonized coconut shell micro and nanocomposites. International Journal of Mechanical and Civil Engineering. 5, 10-24.

Naim Shaik M.B, Arif S, Aziz T, Waseem A, Naim Shaik M.A, and Ali M (2019) Microstructural, mechanical and tribological behavior of powder metallurgy processed SiC and RHA reinforced Al-based composites. Journal of Surfaces and Interfaces 15:166-179.

Oghenevweta JE, and Aigbodion VS (2016) Mechanical properties and microstructural analysis of Al-Si-Mg/carbonized maize stalk waste particulate composites. J King Saud Univ-Eng Sci 28:222-229.

Olaitan S.A (2013) Effect of mahogany filler on mechanical properties of reinforced polyethylene matrix. Acad. Res. Int. 4(4)284-293.

Olaniran O, Oyetunji A, and Oji B (2020) Influence of silicon carbide -CPA weight ratio on the mechanical and tribological characteristics of Al-Mg-Si alloy hybrid composites. Journal of Chemical Technology and Metallutgy. 56(5)1082-1088

Osunmakinde L, Asafa T.B, Agboola P.O, Durowoju M.O (2023) Development of aluminum composite reinforced with selected agricultural residues. Jour of Discover Materials 3(33) https://doi.org/10.1007/s43939-023-00069-z.

Prasad DS, Shoba C, and Ramanaiah N (2014) Investigations on mechanical properties of al hybrid composites. J Mater Res Technol 3:79-85.https://doi.org/10.1016/j.jmrt.2013.11.002.

Prasad, D.V, Shoba, C and Ramanaiah, N (2014). Investigations of mechanical properties of aluminum hybrid composites. J Mater. Res. 3. 79-85.

Saravanan S.D and Kumar M.S (2014) Mechanical behavior of aluminum (AlSi10Mg)-RHA composite. Int. J. Eng. Technol.5:4834-40.

Saravanan S.D, Senthilkumar M, Shankar S (2013) Effect of particle size on tribological behavior of rice husk ash-reinforced aluminum alloy (AlSi10mg) matrix composites. Tribol. Trans. 56:1156-1167, https://doi.org/10.1080/10402004-2013.

Saini S, Gupta A, Mehta A.J, and Pramanik S (2020) Rice husk-extracted silica reinforced graphite/Al-matrix hybrid composite. Journal of Thermal Analysis and Calorimetry https://doi.org/10.1007/s10973-020-10404-8.

Siva Prasad D, and Shoba C (2014) Hybrid composites- a better choice for high wear resistant materials. J. Mater. Res. Technol. 3:172-178. https://doi.org/10.1016/j.jmrt.2014.03.004.

Varalakshmi K, Ch Kishore KK, Ravindra BP, and Ch Sastry MR (2019) Characterization of Al-CSA metal matrix composites using stir casting. Int J Latest Eng. Sci. 2:41-49.

Zuhailawati H, Samayamutthirian P, Haizu CHM, Campus E, Pinang P (2007). Fabrication of low-cost aluminum matrix composite reinforced with silica sand. J Phys Sci 18:47–55.

Virkunwar A.K, Ghosh S, and Basak R (2019) Wear characteristics optimization of Al6061rice husk ash metal matrix composite using Taguchi method. Mater Today Proc 19:546-550https://doi.org/10.1016/j.matpr.2019.07.731.